Higher sensitivity of *Adamts12*-deficient mice to tumor growth and angiogenesis

Mehdi EL HOUR[1], Angela MONCADA-PAZOS[2], Silvia BLACHER[1], Anne MASSET[1], Santiago CAL[2], Sarah BERNDT[1], Julien DETILLEUX[1], Lorin HOST[1], Alvaro J OBAYA[2], Catherine MAILLARD[1], Jean Michel FOIDART[1], Fabien ECTORS[3], Agnès NOEL[1] and Carlos LOPEZ-OTIN[2]

[1]Laboratory of Tumor and Developmental Biology, Groupe Interdisciplinaire de Génoprotéomique Appliquée-Cancer (GIGA-Cancer), University of Liege, B-4000 Liège, Belgium; [2]Departamento de Bioquimica y Biologia Molecular, Universidad de Oviedo, Instituto Universitario de Oncologia, 33006-Oviedo, Asturias, Spain; [3]GIGA-Transgenesis, University of Liege, B-4000 Liège, Belgium.

Running title: Angiogenesis in *ADAMTS12*-deficient mice

Key words: ADAMTS-12, angiogenesis, tumor suppression

Corresponding author: A. NOEL

Laboratory of Tumor and Developmental Biology

University of Liège, Tour de Pathologie (B23)

Sart-Tilman, B-4000 Liège, BELGIUM, Tel: +32-4-366.25.69; Fax: +32-4-366.29.36

E-mail: agnes.noel@ulg.ac.be

Word count: 2335 Abstract (203 words)

Abstract

ADAMTS (A Disintegrin And Metalloproteinase domain with ThromboSpondin motifs) constitute a family of endopeptidases related to matrix metalloproteinases (MMPs). These proteases have been largely implicated in tissue remodelling and angiogenesis associated with physiological and pathological processes. To elucidate the *in vivo* functions of ADAMTS-12, we have generated a knockout mouse strain (*Adamts12*$^{-/-}$) in which *Adamts12* gene was deleted. The mutant mice had normal gestations and no apparent defects in growth, life span and fertility. By applying three different *in vivo* models of angiogenesis (malignant keratinocyte transplantation, Matrigel plug and aortic ring assays) to *Adamts12*$^{-/-}$ mice, we provide evidence for a protective effect of this host enzyme towards angiogenesis and cancer progression. In the absence of Adamts-12, both the angiogenic response and tumor invasion into host tissue were increased. Opposing results were obtained by using medium conditioned by cells overexpressing human ADAMTS-12 which inhibited vessel outgrowth in the aortic ring assay. This angio-inhibitory effect of ADAMTS-12 was independent of its enzymatic activity since a mutated inactive form of the enzyme was similarly efficient in inhibiting endothelial cell sprouting in the aortic ring assay than the wild type form. Altogether, our results demonstrate that ADAMTS-12 displays anti-angiogenic properties and protect the host towards tumor progression.

Introduction

Cancer progression depends not only on the acquisition of new properties by neoplastic cells but also on a complex cross talk occurring between tumor cells and their microenvironment implicating different types of cells, soluble mediators and cell membrane-associated molecules (Nyberg *et al.*, 2008). The contribution of proteolytic enzymes to cancer progression has long been associated with their ability to degrade extracellular matrix components and has been recently extended to their capacity to control the activity and bioavailability of these mediators (Cauwe *et al.*, 2007; Egeblad and Werb, 2002; Overall and Blobel, 2007). Recently, the generation of animal models involving gain or loss of function of matrix metalloproteinases (MMPs) has led to the surprising discovery of tumor-suppressive function for some proteases (Lopez-Otin and Matrisian, 2007). These host protective proteases are not produced by tumor cells, but mainly by tumor infiltrating cells including inflammatory cells (MMP-8) (Balbin *et al.,* 2003) and fibroblastic cells (MMP-19) (Jost *et al.,* 2006). These recent findings have broken the dogma of proteases as simple positive regulators of cancer progression and emphasize the urgent need in identifying individual proteases as host protective partners or tumor-promoting agents.

Among proteases with putative tumor-suppressive functions are the ADAMTS (a disintegrin and metalloproteinase with thrombospondin motifs), matrix metalloproteinase-related enzymes characterized by the presence of at least one thrombospondin type I domain (TSP-1) (Bai *et al.,* 2009; Cal *et al.,* 2001; Porter *et al.,* 2004; Porter *et al.,* 2005). Their multi-domain structure endows these secreted proteins with various functions including the control of cell proliferation, apoptosis, adhesion and migration (Bai *et al.,* 2009; Noel *et al.,* 2008; Rocks *et al.,* 2008). It is worth noting that ADAMTS-1 and ADAMTS-8 display anti-angiogenic properties (Liu *et al.,* 2006; Vazquez *et al.,* 1999). Our recent studies have highlighted the anti-tumor properties exhibited by ADAMTS-12 (Cal *et al.,* 2001; Llamazares *et al.,* 2007). In accordance with this

concept of ADAMTS-12 being a host protective enzyme, *ADAMTS12* is epigenetically silenced in human tumor samples and tumor cell lines (Moncada-Pazos *et al.,* 2009). However, the exact contribution of ADAMTS-12 during the different steps of cancer progression including angiogenesis remains to be elucidated. To address this important issue, we have generated mutant mice lacking *Adamts12* gene. *Adamts12*-deficiency did not cause obvious abnormalities during embryonic development or in adult mice. Therefore, mutant mice provide a novel and useful tool to investigate Adamts-12 functions in pathological angiogenesis. Through different complementary approaches, we provide evidence that Adamts-12 protects the host against tumor angiogenesis, growth and invasion.

Results

Adamts12-deficient mice are viable without any obvious phenotype

The biological functions of ADAMTS-12, a metalloprotease-related enzyme overexpressed in human cancers (Porter *et al.* 2004), are poorly understood. To establish a mutant mouse strain deficient for *Adamts12* gene (KO, *Adamts12*$^{-/-}$ mice), the targeting vector was designed in order to replace the exons 6 and 7 (corresponding to the N-terminal part of the catalytic domain) by a NEO-PGK cassette (Fig. 1A). ES clones generated by homologous recombination (Fig.1B) were injected into C57Bl/6J blastocysts to generate chimeric males. Heterozygous mice from the F1 generation were intercrossed to generate *Adamts12*-deficient mice that were obtained in the Mendelian ratio. We checked mice genotypes by PCR (Fig. 1C).

The expression of *Adamts12* was determined by RT-PCR in different organs. In WT mice, *Adamts12* was expressed in some organs including ovary, mammary gland, uterus, lung, ear cartilage and lymph node (Fig. 1D). *Adamts12* was not expressed in heart, kidney, bone, liver, brain, intestine, testis, muscle, skin, eyes and spleen (data not shown). As expected, tissues from *Adamts12*$^{-/-}$ mice did not produce any *Adamts12* in all organs tested, as assessed by RT-PCR amplification using primers targeting the catalytic domain (Fig.1D) and the pro-domain (data not shown). Despite *Adamts12*-deficiency, mutant mice developed normally, were fertile and had long-term survival rates indistinguishable from those of their wild type counterpart. No obvious phenotype was detected. These findings clearly indicate that *Adamts12* is dispensable for embryonic and adult mouse development and growth.

Adamts12-deficiency affects tumoral angiogenesis

In the course of the phenotyping of *Adamts12*$^{-/-}$ mice, we evaluated its expression in pathological conditions. *Adamts12* expression was first investigated during laser-induced choroidal

neovascularization by RT-PCR analyses performed at various time points after laser burn (Lambert *et al.,* 2003). *Adamts12* expression was never detected at any stage of choroidal neovascularization (data not shown), excluding the potential implication of Adamts-12 in choroidal angiogenesis.

The overexpression of *ADAMTS12* in various human cancers (Cal *et al.,* 2001) prompted us to explore its putative functions in tissue remodelling associated with cancer development. We applied three models of angiogenesis which have been previously successfully used to evaluate the contribution of different metalloproteinases during angiogenic processes (Berndt *et al.,* 2006; Berndt *et al.,* 2008; Masson *et al.,* 2002). The transplantation system is a highly sensitive tool to inspect the kinetic of early steps of host stromal response to tumor signals (Jost *et al.,* 2007; Jost *et al.,* 2004; Mueller *et al.,* 2004). Malignant murine PDVA keratinocytes precultured on a type I collagen gel were transplanted onto wild-type (*n*=14) and *Adamts12*-deficient mice (n=14). An early endothelial cell migration towards the tumor layer can be visualized through double immunostaining carried out to distinguish tumor cells (keratin positive) and vessels (cD31 positive cells or type IV collagen positive basement membrane) (Blacher *et al.,* 2008). Two different patterns of invasion were observed 21 days after transplantation (Fig. 2). A low vascularized profile scored + was characterized by blood vessel infiltration of the collagen gel without reaching the tumor layer. Then, once blood vessels have reached tumor cell layers, malignant keratinocytes formed tumor sprouts that invaded downwards the remodelled host tissue and were intermingled with new vessels (Fig. 2). Such highly vascularized pattern was scored +++. Tumor vascularization and invasion was improved in *Adamts12*$^{-/-}$ mice. Indeed, 86% of transplants were highly vascularized (scored +++), while 14% of samples were scored +. In WT mice, the percentage of transplants scored +++ fell down to 57% and that of low vascularized transplants reached 43% (P=0.027, χ^2 test) (Fig. 2A, B).

To further confirm this distinct invasive profile, an original method of computerized image analysis (Blacher *et al.,* 2008) allowing a concomitant quantification of blood vessel recruitment and tumor cell invasion was applied to all samples. The distribution of tumor cell and endothelial cell densities were determined as a function of distance to the top of the tumor (Fig. 2C, D). With this aim, a grid formed from the dilatation of tumor boundaries was superposed onto tumor and vascularization images as described previously (Blacher *et al.,* 2008). The degree of superimposition of curves corresponding to vessel and tumor densities determines tumor vascularization. Yellow spots in Fig. 2 delineate areas of tumor in which tumor cells and blood vessels were intermingled, reflecting tumor vascularization. In *Adamts12*$^{-/-}$ mice, invasion and migration process took place to a much larger extent (Fig. 2C, D; $P<0.05$). A stronger invasion characterized by a deeper extension of tumor cells was observed in *Adamts12*$^{-/-}$ mice (migration up to Lmax = 3.55 ± 0.4 mm in KO mice *versus* Lmax = 2.5 ± 0.4 mm in WT mice, $P<0.05$, Mann-Whitney test). In addition, blood vessels migrated roughly towards tumor cells leading to increased overlapping area of tumor cells and blood vessels (Fig. 2C, D, yellow spot). Indeed, the area of vessels intermingled with tumor cells was twice higher in mutant mice (0.27 mm^2 *versus* 0.13 mm^2 in WT mice).

These data indicate that *Adamts12*-deficiency in host tissue is associated with an acceleration of the angiogenic response and increased tumor invasion into the host tissue. It is worth noting that malignant keratinocytes used in this model did not express *Adamts12 in vitro*, while human ADAMTS-12 was detected in tumor transplants. This suggests an induction of host expression following tumor cell transplantation *in vivo*. These data are in line with our recent study showing that *ADAMTS12* expression by fibroblasts is enhanced in co-culture with cancer cells (Moncada-Pazos *et al.,* 2009). They are also in full agreement with a previous report showing that *ADAMTS12* as other family members (*ADAMTS2, 7, 8* and *10*) are predominantly expressed in

stromal fibroblasts from human mammary tissues, but not in breast cancer cells (Porter *et al.*, 2004). Altogether, these observations suggest that fibroblastic cells are an important source of ADAMTS-12 and respond to the presence of tumor cells by producing this enzyme.

Adamts-12 affects in vivo and ex vivo angiogenesis

The angiogenic response to basic Fibroblast Growth Factor (bFGF) was then investigated in WT and mutant mice. Matrigel (500µl) containing heparin (10U/ml) and bFGF (250ng/ml) were injected subcutaneously into mice (n=16). To quantify functional vessel recruitment, hemoglobin concentrations were measured in the plugs harvested 7 days after injection (Berndt *et al.*, 2006). The angiogenic response induced by bFGF was again higher in *Adamts12*$^{-/-}$ than in WT mice. In WT mice, the mean hemoglobin content was 2-fold reduced (0.65±0.1 Hb (mg/ml)/mg of plug in WT mice *versus* 1.65±0.5 Hb (mg/ml)/mg of plug in *Adamts12*$^{-/-}$ mice), and the percentage of poorly vascularized plugs (hemoglobin concentration lower than 0.5 Hb(mg/ml)/mg of plug) reached 56% (9/16) in WT mice, while it was less than 12% (2/16) in mutant mice ($P<0.05$).

To further study the contribution of Adamts-12 in neovessel formation, aortic explants issued from mutant or WT mice were embedded into a 3D-type I collagen gel in the presence of serum corresponding to their genotype (Fig. 3A). An increased angiogenic response was observed in *Adamts12*$^{-/-}$ mice as evidenced by increased sprout density (Fig. 3B, left graph) and vessel length (Fig. 3B, right graph). Since the formation of capillary-like structures is associated with the spreading out of mural cells, we performed immunohistochemical labelling on whole mount of aortic rings. Interestingly, increased mural cell recruitment detected by NG2 labelling was observed in IB4 positive capillaries issued from *Adamts12*$^{-/-}$ mice (Fig. 3C). Computerized quantification revealed that the mean area of co-localisation between IB4 positive endothelial

cells and NG2 positive mural cells was twice higher in sprouts issued from *Adamts12*$^{-/-}$ mice as compared to those from WT explants (Fig. 3D). These data reflect an increased maturation of blood vessels in the absence of Adamts-12. Altogether these findings indicate that *ADAMTS12* is a negative regulator of angiogenesis.

The finding that *Adamts12*-deficiency resulted in an acceleration of the angiogenic response led us to postulate that cells overexpressing ADAMTS-12 would have opposite effect and would inhibit it. To address this question, we next evaluated the impact of medium conditioned by a population of MCF7 cells overexpressing human FLAG-tagged-ADAMTS-12 (MCF7p ADAMTS-12 FLAG) on neovessel formation in another experimental model using aortic rings issued from a rat. The presence of ADAMTS-12 in the conditioned media was assessed by Western blot (data not shown) using an anti-FLAG antibody allowing the detection of a specific band of molecular mass ≈ 175kDa. In accordance to our hypothesis, the medium of cells overexpressing ADAMTS-12 inhibited the angiogenic response as revealed by a reduction vessel length (Fig. 4B) and vessel maturation through pericyte coverage (Fig. 4C).

We next determined whether the anti-tumorigenic effect of ADAMTS-12 could be ascribed to its catalytic function. With this aim, new MCF7 transfectants were generated to produce inactive mutants of ADAMTS-12 or intact ADAMTS-12. Point mutations of two key amino acids of the catalytic site (H465Q/E466A) were performed as previously described (Cal *et al.,* 2001). These mutations in the catalytic domain did not impair the anti-angiogenic effect induced by medium conditioned by transfectants (Fig. 4 D, E). Indeed, the medium conditioned by cells overexpressing intact ADAMTS-12 or mutated ADAMTS-12 inhibited the spreading out of endothelial cells as assessed by a reduction of vessel length (Fig. 4D) and of vessel maturation through pericyte coverage (Fig. 4E). These results suggest that the catalytic activity of ADAMTS-12 is dispensable for its angioinhibitory function.

Our data are in line with our previous report showing that ADAMTS12 inhibits the formation of VEGF-induced tubular structures in BAE-1 cells (Llamazares *et al.,* 2007). The finding of anti-angiogenic effects for a member of the ADAMTS family is not unprecedented as it has also been described for ADAMTS-1 and ADAMTS-8 (Dunn *et al.,* 2006; Vazquez *et al.,* 1999). However, the originality of our findings relies on the identification of a key host ADAMTS12 contribution in the host protection towards the angiogenic response induced by tumor cells. This report based on the generation of a novel loss-of-function animal model provides the first demonstration of the anti-angiogenic properties of a single host ADAMTS. Moreover, in contrast to ADAMTS-1 whose proteolytic activity is apparently required for its anti-angiogenesis property (Iruela-Arispe *et al.,* 2003), the angioinhibitory property of ADAMTS12 does not depend on its catalytic activity. We cannot ruled out the possibility that ADAMTS12 can sequester VEGF through its C-terminal TSP domain(s) and the spacer region as previously described for ADAMTS-1 (Luque *et al.,* 2003). Addressing this issue would require a carefull dissection of the complex C-terminal part of ADAMTS-12 containing seven TSP repeats, two spacers and a PLAC domain which is out of the scope of the present study.

In conclusion, we propose that the ADAMTS-12 production induced in response to the presence of cancer cells could have a beneficial protective effect towards tumor growth and invasion. The new generation of *Adamts12*-deficient mice provides a suitable tool to give new insights into the *in vivo* functions of this enzyme which are presently unknown. In addition, this new transgenic tool paves the way for further investigations on the biological functions of ADAMTS-12 in various pathological conditions in which the enzyme is putatively involved such as asthma (Kurz *et al.,* 2006) and arthritis (Bai *et al.,* 2006).

CONFLICT OF INTEREST

The authors declare no conflict of interest.

ACKNOWLEDGMENTS

The authors acknowledge F. Olivier and G. Roland for their excellent technical assistance. This work was supported by grants from Ministerio de Ciencia e Innovación, Fundación M. Botin, European projects (FP7 HEALTH-F2-2008-201279 “MICROENVIMET”), the Fondation contre le Cancer, the D.G.T.R.E. from the « Région Wallonne », the Interuniversity Attraction Poles Programme - Belgian Science Policy (Belgium). MEH, AM, JD, LH and FE are recipients of grants from the Fonds National de la Recherche Scientifique (FNRS, Belgium).

REFERENCES

Bai XH, Wang DW, Luan Y, Yu XP, Liu CJ. (2009). Regulation of chondrocyte differentiation by ADAMTS-12 metalloproteinase depends on its enzymatic activity. *Cell Mol Life Sci* **66**: 667-680.

Balbin M, Fueyo A, Tester AM, Pendas AM, Pitiot AS, Astudillo A, *et al.* (2003). Loss of collagenase-2 confers increased skin tumor susceptibility to male mice. *Nat Genet* **35**: 252-257.

Berndt S, Bruyere F, Jost M, Edwards DR, Noel A. (2008). *In vitro* and *in vivo* models of angiogenesis to dissect MMP functions. In Edwards DR, Hoyer-Hansen G, Blasi F, Sloane BF. (Eds.). *The Cancer Degradome: Proteases and Cancer Biology*: 305-325. New-York: Springer.

Berndt S, Perrier DS, Blacher S, Pequeux C, Lorquet S, Munaut C, *et al.* (2006). Angiogenic activity of human chorionic gonadotropin through LH receptor activation on endothelial and epithelial cells of the endometrium. *FASEB J.* **20**: 2630-2632.

Blacher S, Jost M, Melen-Lamalle L, Lund LR, Romer J, Foidart JM, *et al.* (2008). Quantification of in vivo tumor invasion and vascularization by computerized image analysis. *Microvasc Res* **75**: 169-178.

Cal S, Arguelles JM, Fernandez PL, Lopez-Otin C. (2001). Identification, characterization, and intracellular processing of ADAM-TS12, a novel human disintegrin with a complex structural organization involving multiple thrombospondin-1 repeats. *J Biol Chem* **276**: 17932-17940.

Cauwe B, Van den Steen PE, Opdenakker G. (2007). The biochemical, biological, and pathological kaleidoscope of cell surface substrates processed by matrix metalloproteinases. *Crit Rev Biochem Mol Biol* **42**: 113-185.

Dunn JR, Reed JE, du Plessis DG, Shaw EJ, Reeves P, Gee AL *et al.* (2006). Expression of ADAMTS-8, a secreted protease with antiangiogenic properties, is downregulated in brain tumours. *Br J Cancer* **94**: 1186-1193.

Egeblad M, Werb Z. (2002). New functions for the matrix metalloproteinases in cancer progression. *Nat Rev Cancer* **2**: 161-174.

Iruela-Arispe ML, Carpizo D, Luque A. (2003). ADAMTS1: a matrix metalloprotease with angioinhibitory properties. *Ann N Y Acad Sci* 995: 183-190.

Jost M, Folgueras AR, Frerart F, Pendas A, Blacher S, Houard X *et al.* 2006. Earlier onset of tumoral angiogenesis in matrix metalloproteinase-19-deficient mice. *Cancer Res* **66**: 5234-5241.

Jost M, Maillard C, Lecomte J, Lambert V, Tjwa M, Blaise P *et al.* (2007). Tumoral and choroidal vascularization: differential cellular mechanisms involving plasminogen activator inhibitor type I. *Am J Pathol* **171**: 1369-1380.

Jost M, Vosseler S, Blacher S, Fusenig NE, Mueller MM, Noel A. (2008). The surface transplantation model to study the tumor-host interface. In Edwards, D. R., Hoyer-Hansen, G., Blasi, F., & Sloane, B. F. (Eds.), *The Cancer Degradome: Proteases and Cancer Biology*: 327-342. New-York: Springer.

Kurz T, Hoffjan S, Hayes MG, Schneider D, Nicolae R, Heinzmann A *et al.* (2006). Fine mapping and positional candidate studies on chromosome 5p13 identify multiple asthma susceptibility loci. *J Allergy Clin Immunol* **118**: 396-402.

Lambert V, Wielockx B, Munaut C, Galopin C, Jost M, Itoh T *et al.* (2003). MMP-2 and MMP-9 synergize in promoting choroidal neovascularization. *FASEB J* **17**: 2290-2292.

Liu YJ, Xu Y, Yu Q. (2006). Full-length ADAMTS-1 and the ADAMTS-1 fragments display pro- and antimetastatic activity, respectively. *Oncogene* **25**: 2452-2467.

Llamazares M, Obaya AJ, Moncada-Pazos A, Heljasvaara R, Espada J, Lopez-Otin C *et al.* (2007). The ADAMTS12 metalloproteinase exhibits anti-tumorigenic properties through modulation of the Ras-dependent ERK signalling pathway. *J Cell Sci* **120**: 3544-3552.

Lopez-Otin C, Matrisian LM. (2007). Emerging roles of proteases in tumour suppression. *Nat Rev Cancer* **7**: 800-808.

Luque A, Carpizo DR, Iruela-Arispe ML. (2003). ADAMTS1/METH1 inhibits endothelial cell proliferation by direct binding and sequestration of VEGF165. *J Biol Chem* **278**: 23656-23665.

Masson VV, Devy L, Grignet-Debrus C, Bernt S, Bajou K, Blacher S, *et al.* (2002). Mouse Aortic Ring Assay: A New Approach of the Molecular Genetics of Angiogenesis. Biol Proced Online **4**: 24-31.

Moncada-Pazos A, Obaya AJ, Fraga MF, Viloria CG, Capella G, Gausachs M *et al.* (2009). The ADAMTS12 metalloprotease gene is epigenetically silenced in tumor cells and transcriptionally activated in the stroma during progression of colon cancer. *J Cell Sci* **122**: 2906-2913.

Mueller MM, Fusenig NE. (2004). Friends or foes - bipolar effects of the tumour stroma in cancer. *Nat Rev Cancer* **4**: 839-849.

Noel A, Jost M, Maquoi E. (2008). Matrix metalloproteinases at cancer tumor-host interface. *Semin Cell Dev Biol* **19**: 52-60.

Nyberg P, Salo T, Kalluri R. (2008). Tumor microenvironment and angiogenesis. *Front Biosci* **13**: 6537-6553.

Overall CM, Blobel CP. (2007). In search of partners: linking extracellular proteases to substrates. *Nat Rev Mol Cell Biol* **8**: 245-257.

Porter S, Clark IM, Kevorkian L, Edwards DR. (2005). The ADAMTS metalloproteinases. Biochem J **386**: 15-27.

Porter S, Scott SD, Sassoon EM, Williams MR, Jones JL, Girling AC *et al.* (2004). Dysregulated expression of adamalysin-thrombospondin genes in human breast carcinoma. *Clin Cancer Res* **10**: 2429-2440.

Rocks N, Paulissen G, El Hour M, Quesada F, Crahay C, Gueders M *et al.* (2008). Emerging roles of ADAM and ADAMTS metalloproteinases in cancer. *Biochimie* **90**: 369-379.

Vazquez F, Hastings G, Ortega MA, Lane TF, Oikemus S, Lombardo M *et al.* (1999). METH-1, a human ortholog of ADAMTS-1, and METH-2 are members of a new family of proteins with angio-inhibitory activity. *J Biol Chem* **274**: 23349-23357.

Legends of figures:

Figure 1. Targeted disruption of mouse *Adamts12* gene. A: Schematic illustration of the targeting strategy (top, wild-type allele; bottom: targeted allele). A genomic clone encoding *Adamts12* was obtained from a mice 129/SvJ strain genomic DNA library. The exons 6 and 7 were replaced by a neomycin-phosphoglycerate kinase (NEO-PGK) cassette.Predicted sizes of Xho I fragments are indicated. (Rectangle = exon; double headed arrows: probes for detecting the homologous recombination event). B: Xho I Southern Blot analysis of +/+ and +/- ES129 cells. The targeted embryonic stem (ES) clones obtained by homologous recombination were then injected into blastocysts (10 to 15 cells per blastocyst of day 4). C: Example of PCR genotyping from tail biopsies of *Adamts12* WT (+/+), *Adamts12* heterozygous (+/-) and homozygous *Adamts12* (-/-) mice generated in C57BL/6 genetic background. (D) RT-PCR analysis of *Adamts12* expression in WT and KO mouse tissues. Positive controls are Embryo (E) and placenta (P). Representative gels are displayed with the expected size (bp) of RT-PCR products on the right.

Figure 2. Histological analysis of tumor transplanted into mice. Malignant murine PDVA keratinocytes precultured on a collagen gel were covered by a silicone chamber and transplanted for three weeks on the back of 6- to 8-week-old mice *Adamts12*$^{+/+}$ (WT) (A,C) or *Adamts12*$^{-/-}$ (KO) (B,D) mice (n = 14 per experimental groups). A, B: Double immunostaining were carried out on cryostat section to identify tumor cells (anti-keratin antibody, green) and vessels (anti-type IV collagen or anti-CD31, red). Magnification, 40-fold. Bar, 0.5mm. C,D: Tumor and endothelial cell density distributions determined by computerized image analysis. After image binarization/segmentation, the upper boundary of the tumor was automatically detected and a grid

was constructed with the successive dilations (n=1, 2, 3….) of this upper boundary. Tumor and vessel densities were determined on each interval of the grid. Results were drawn in function of the distance to the upper tumor limit. Intermingling of tumor cells and vessels is shown by superimposition of the respective curves (yellow areas). The maximal distance of tumor cell invasion (Lmax) is indicated by an arrow head.

Figure 3: Capillary outgrowth from mouse aortic rings cultured in a collagen gel. A: Morphological observation of explants of mouse thoracic aorta issued from *Adamts12*$^{+/+}$ (WT) and *Adamts12*$^{-/-}$ mice (KO). Magnification 25-fold. Bar, 1mm. B: Computerized quantification. Two parameters are shown: number (left graph) and maximal length of vessels (right graph). **: $P<0.01$ (Mann-Whitney test). C: Characterization of cells spreading out of aortic rings. Immunostainings were performed on whole mount rings to identify endothelial cells (IB4, green), pericytes (anti-NG2 antibody, red) and pericytes covering endothelial cells (IB4+NG2, merged in yellow). Magnification 40-fold. Bar, 0.5mm. D: The area of colocalization (mm^2) between pericytes and endothelial cells was determined by using a computer-assisted method. *: $P<0.05$ (Mann-Whitney test).

Figure 4: Capillary outgrowth from rat aortic rings cultured in the presence of ADAMTS-12. Wistar rat aortic explants were cultured in MCDB-131 medium (2.5ml) supplemented with medium (2.5ml) conditioned by a population of MCF7 cells expressing (MCF7pADAMTS12-FLAG) or not (MCF7pCONTROL-FLAG) tagged-ADAMTS12. A: Morphological observation of aortic explants in the absence of ADAMTS-12 (MCF7pCONTROL-FLAG) or in the presence of ADAMTS-12 (MCF7pADAMTS-12-FLAG). Magnification 25-fold. Bar,1mm. B: Maximal length of vessels was quantified by computerized image analysis. C: Area of colocalization

(mm^2) of pericytes and endothelial cells was determined by using a computer-assisted method applied to immunostainings performed on whole mounts (see legend of figure 3). D-E: Impact of point mutation of ADAMTS-12 catalytic site. Populations of MCF7 cells expressing wild type ADAMTS12 (MCF7pADAMTS12), inactive mutant ADAMTS-12 (MCF7pH465Q/E466A) or not expressing ADAMTS12 (MCF7pCONTROL) were generated by stable transfection and their conditioned media were tested in the rat aortic ring assay. The double point mutation in the catalytic site did not affect the inhibitory effect of ADAMTS12 on vessel sprouting (D) and on vessel coverage by pericytes (E). Similar results were obtained with two clones of each transfectants. *: $P<0.05$; ***: $P<0.001$ (Mann-Whitney test).

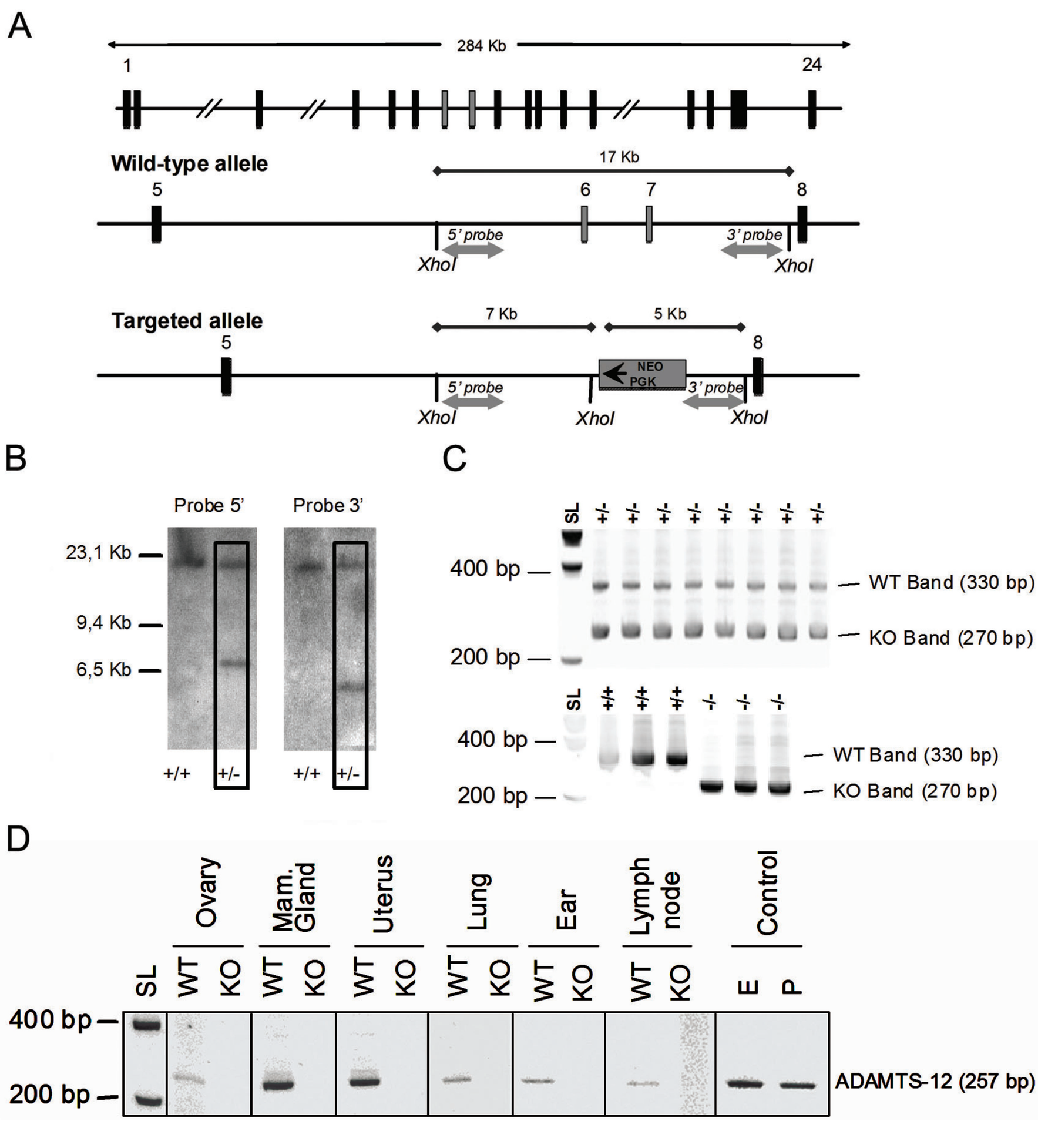
A
284 Kb
1
24
Wild-type allele
17 Kb
5
6
7
8
5' probe
3' probe
XhoI
XhoI
Targeted allele
7 Kb
5 Kb
5
8
NEO
PGK
5' probe
3' probe
XhoI
XhoI
XhoI
B
Probe 5'
Probe 3'
23,1 Kb
9,4 Kb
6,5 Kb
+/+
+/-
+/+
+/-
C
SL
+/-
+/-
+/-
+/-
+/-
+/-
+/-
+/-
400 bp
200 bp
WT Band (330 bp)
KO Band (270 bp)
SL
+/+
+/+
+/+
-/-
-/-
-/-
400 bp
200 bp
WT Band (330 bp)
KO Band (270 bp)
D
SL
Ovary
WT
KO
Mam. Gland
WT
KO
Uterus
WT
KO
Lung
WT
KO
Ear
WT
KO
Lymph node
WT
KO
Control
E
P
400 bp
200 bp
ADAMTS-12 (257 bp)

Figure 1

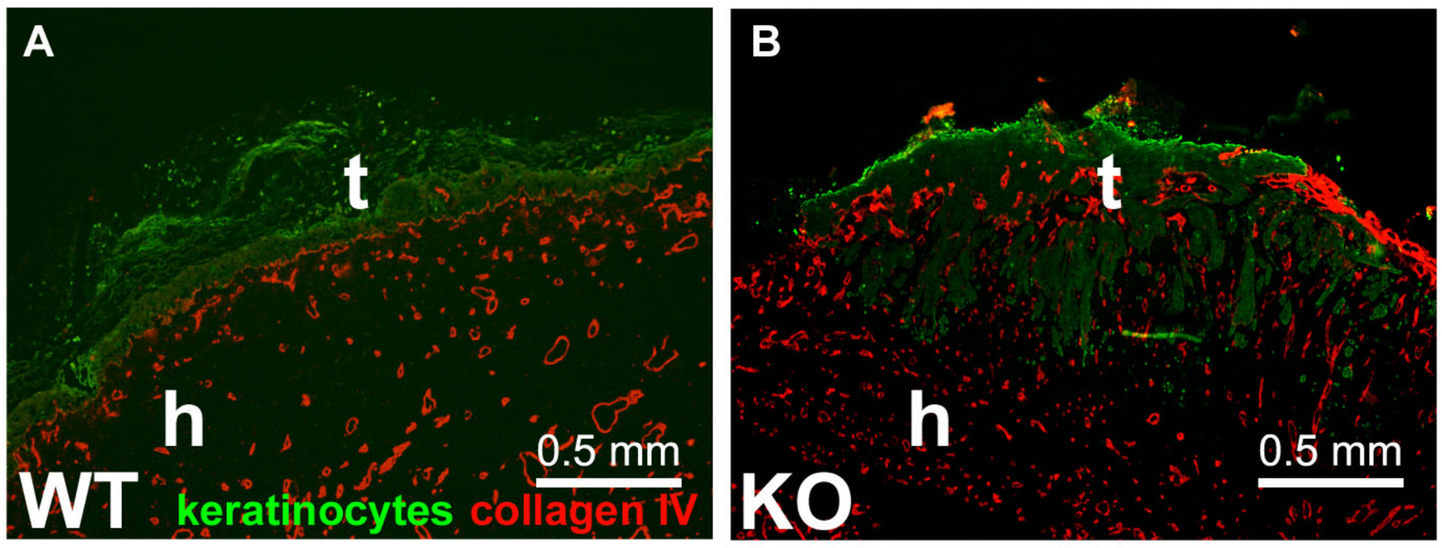
A
t
h
0.5 mm
WT
keratinocytes
collagen IV
B
t
h
0.5 mm
KO

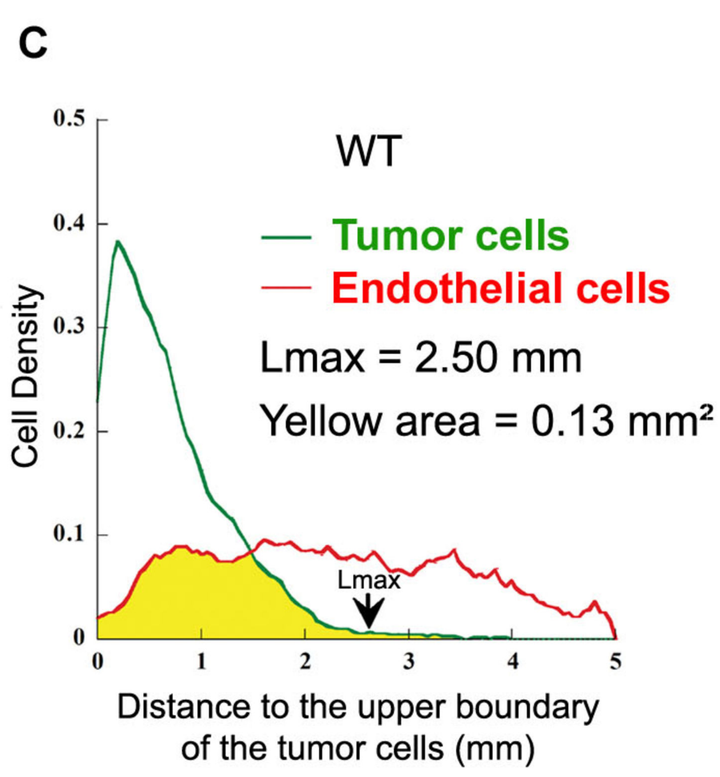
C
WT
Tumor cells
Endothelial cells
Lmax = 2.50 mm
Yellow area = 0.13 mm²
Lmax
Cell Density
0.5
0.4
0.3
0.2
0.1
0
0
1
2
3
4
5
Distance to the upper boundary
of the tumor cells (mm)

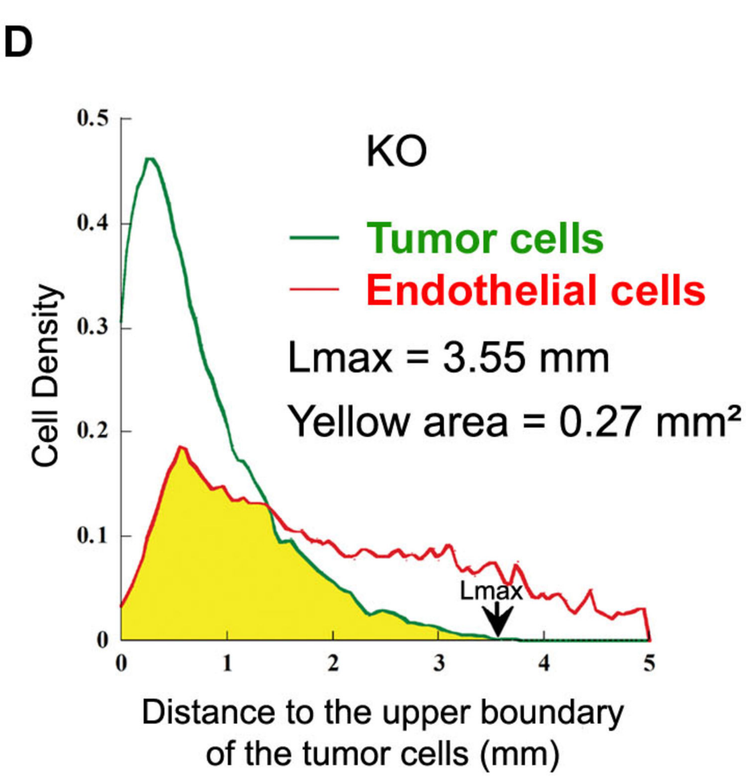
D
KO
Tumor cells
Endothelial cells
Lmax = 3.55 mm
Yellow area = 0.27 mm²
Lmax
Cell Density
0.5
0.4
0.3
0.2
0.1
0
0
1
2
3
4
5
Distance to the upper boundary
of the tumor cells (mm)

Figure 2

A

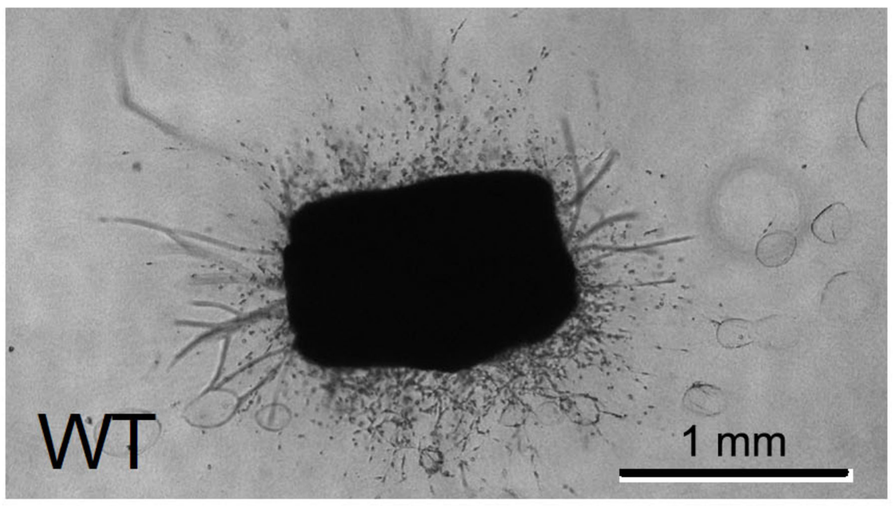

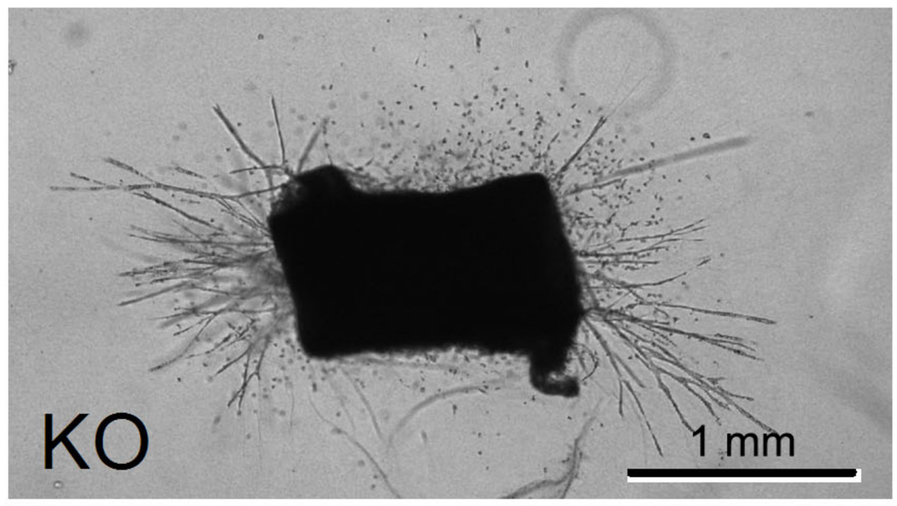

B

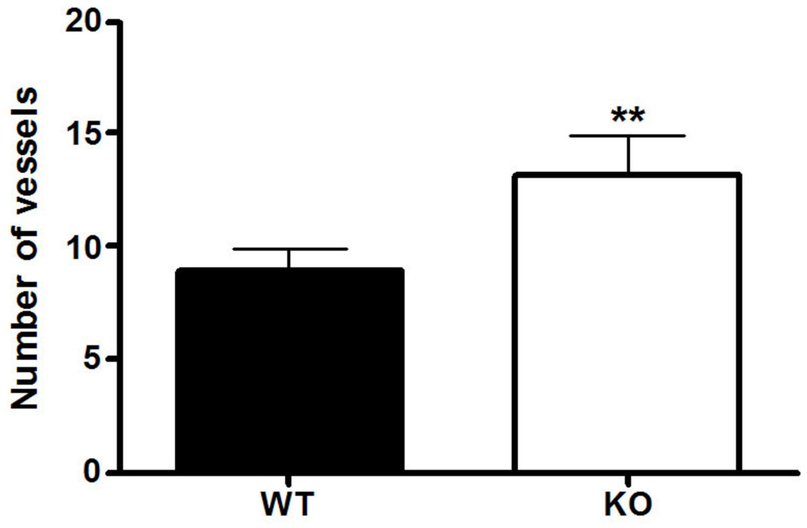

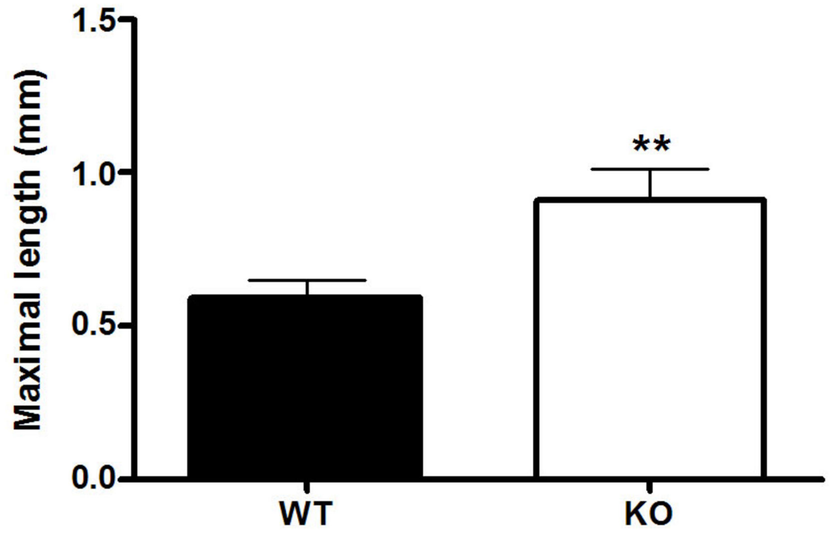

C

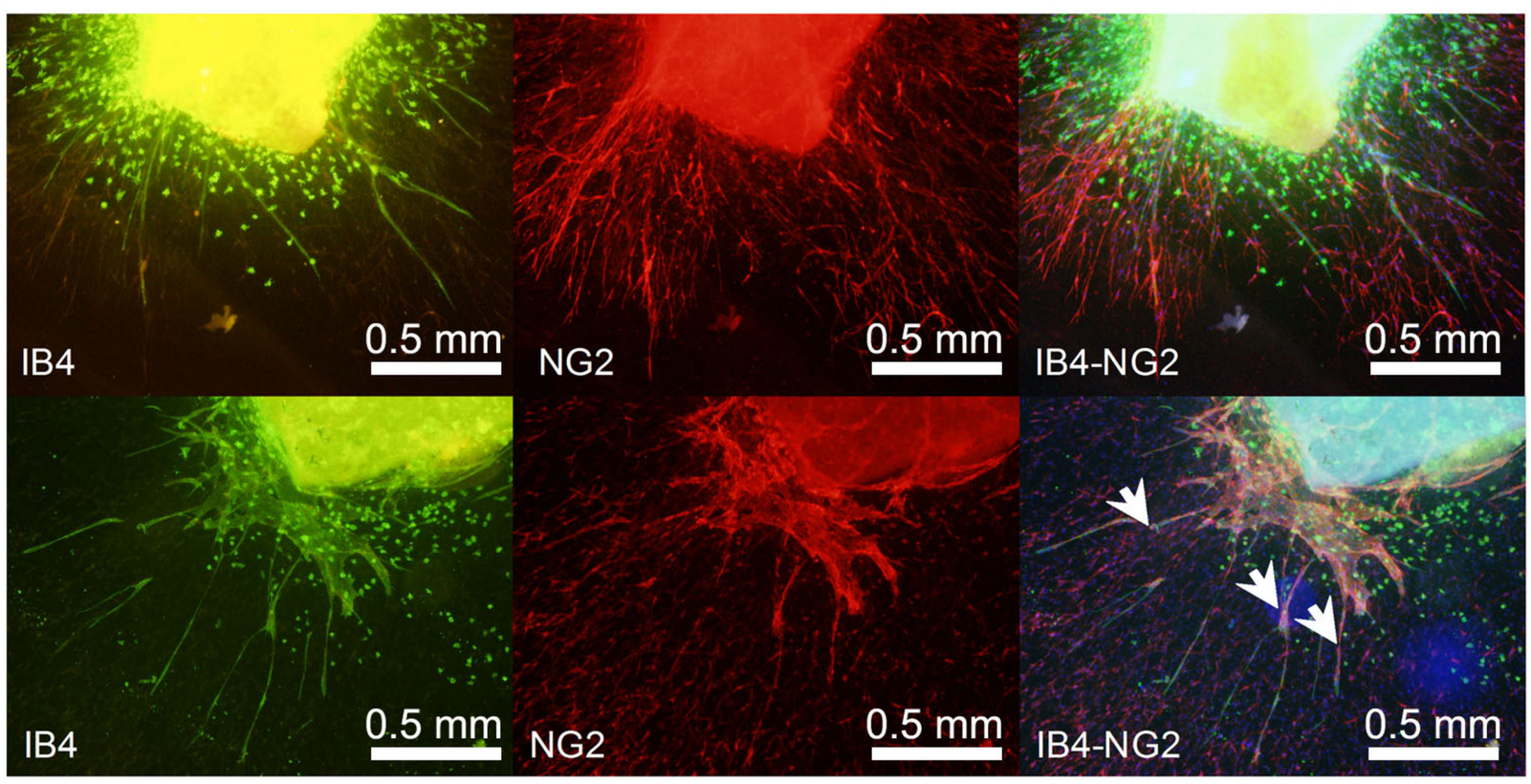

D

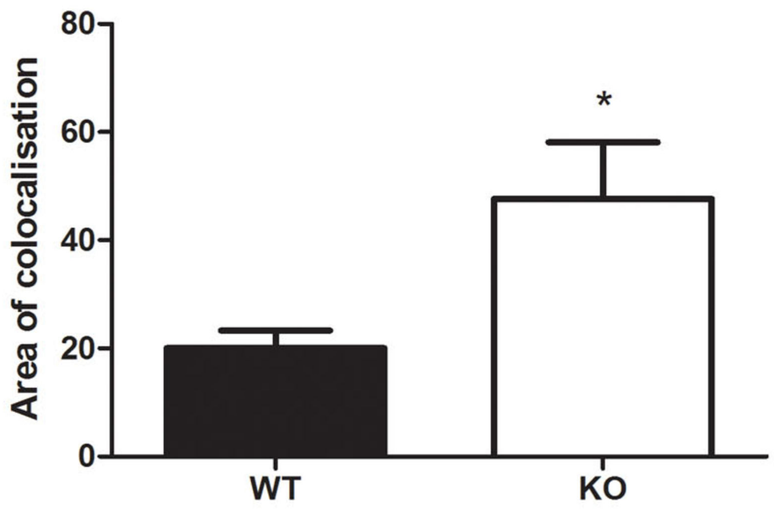

Figure 3

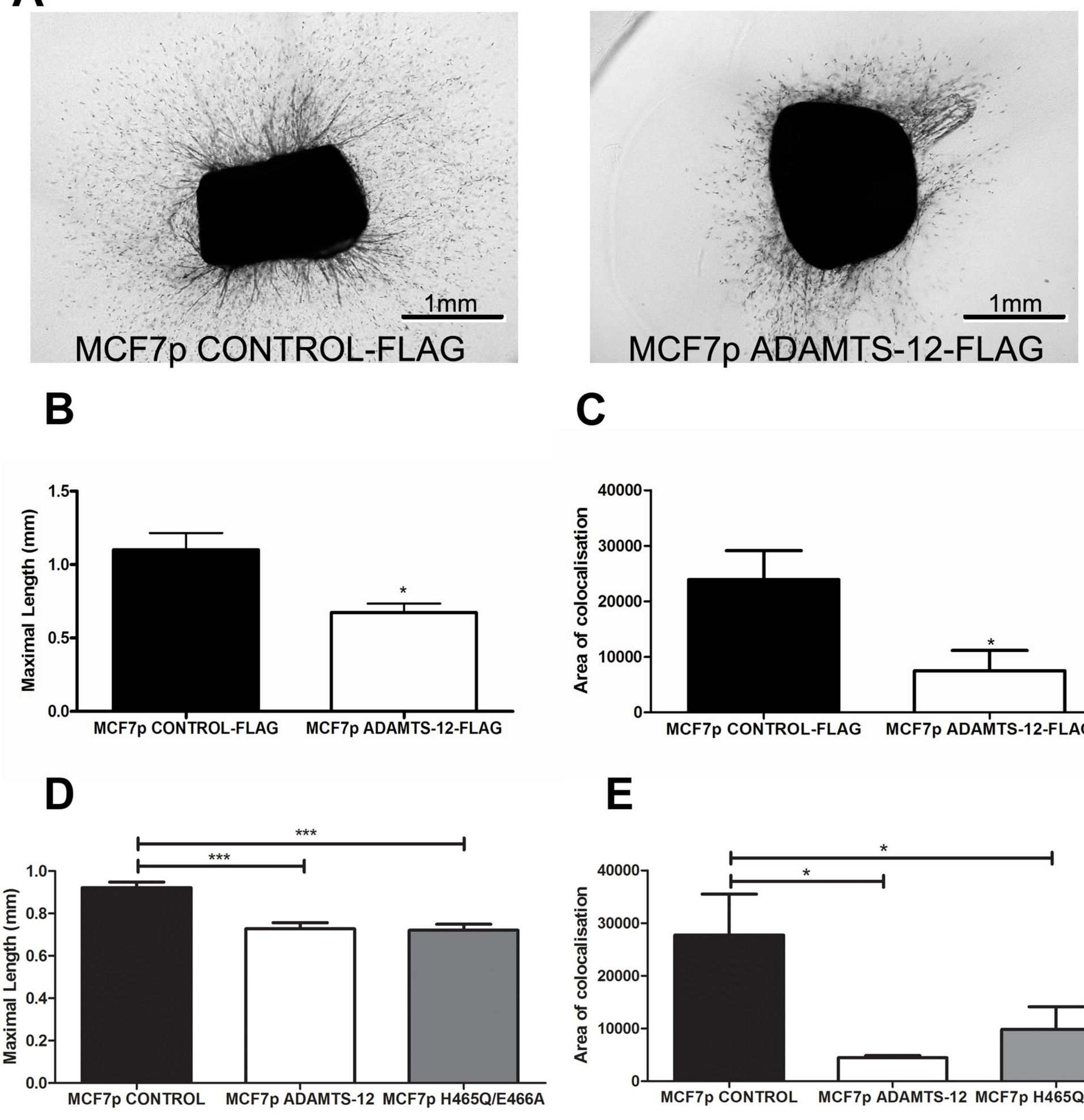
A
1mm
MCF7p CONTROL-FLAG
1mm
MCF7p ADAMTS-12-FLAG
B
Maximal Length (mm)
1.5
1.0
0.5
0.0
*
MCF7p CONTROL-FLAG
MCF7p ADAMTS-12-FLAG
C
Area of colocalisation
40000
30000
20000
10000
0
*
MCF7p CONTROL-FLAG
MCF7p ADAMTS-12-FLAG
D
***
***
Maximal Length (mm)
1.0
0.8
0.6
0.4
0.2
0.0
MCF7p CONTROL
MCF7p ADAMTS-12
MCF7p H465Q/E466A
E
*
*
Area of colocalisation
40000
30000
20000
10000
0
MCF7p CONTROL
MCF7p ADAMTS-12
MCF7p H465Q/E466A

Figure 4